

Free-standing NiCo₂S₄@VS₂ nanoneedle array composite electrode for high performance asymmetric supercapacitor application

Zhiguo Zhang^a, Xiao Huang^a, Hongxia Wang^b, Siow Hwa Teo^a, Tingli Ma^{a,c*}

^a Department of Life Science and System Engineering, Kyushu Institute of Technology, Kitakyushu 8080134, Japan.

^b School of Chemistry, Physics and Mechanical Engineering, Queensland University of Technology, Brisbane, QLD 4001, Australia

^c School of Petroleum and Chemical Engineering, Dalian University of Technology, Dalian 124221, Liaoning China.

* Corresponding author. Email: tinglima@life.kyutech.ac.jp (T. Ma).

ABSTRACT

The growth of two-dimensional (2D) VS₂ nanosheets along the NiCo₂S₄ needle arrays was prepared via an in situ sulfurization-assisted hydrothermal process. The binder-free NiCo₂S₄@VS₂ supercapacitor electrode has contributed to a high specific capacity of 1023.4 mAh g⁻¹, which is 1.7-fold higher than NiCo₂S₄ and 9.8-fold higher than VS₂ electrode under the current density of 0.45 A g⁻¹ in a three-electrode system. Additionally, the NiCo₂S₄@VS₂ supercapacitor electrode exhibited remarkable cyclic stability where 96% of its capacity retained after 2000 cycles. Promoting for real supercapacitor applications, an asymmetric supercapacitor (ASC) composed of NiCo₂S₄@VS₂ as the positive electrode and activated carbon (AC) as the negative electrode with polypropylene as the separator was fabricated. The assembled ASC contributed to a maximum energy density of 31.2 Wh kg⁻¹ at the power density of 775 W kg⁻¹ with good stabilities under different current densities during the cycling test. Thereby, this design of free-standing NiCo₂S₄@VS₂ nanocomposite provides a new strategy for synthesizing efficient electrode materials for high-performance supercapacitors.

Keywords: NiCo₂S₄@VS₂; unique nano structure; binder-free; asymmetric supercapacitor

1. Introduction

The depletion of fossil fuels and skyrocketing environmental issues have urged the needs for sustainable and green energy sources for the development of electronic devices and applications[1, 2]. Among the energy conversion and storage appliances, supercapacitors (SCs) have attracted considerable attention as one of the promising energy storage devices owing to their merits such as environment-benign, low-cost, long-cycle life and good safety over a broad temperature range[3-7]. Furthermore, SCs possess higher power density than batteries and larger energy density than traditional metal plate based electrostatic capacitors. So far, commercial SCs which employ carbon as the electrode material have been used in portable devices and vehicle systems[8, 9]. Nevertheless, the limited energy density of SCs, as compared to batteries impedes their widespread applications[8, 10-13]. Thus, relentless efforts have been devoted to increase the energy density of SCs by tailoring the electrolyte and electrode materials used in SCs to enhance the operational potential window and material capacity[3, 14]. For instance, although the organic electrolytes exhibit a larger stable potential window than aqueous based electrolyte, nevertheless, the poor conductivity, toxicity and high cost of organic electrolytes may restrict their usage in large scale SCs applications[15]. Alternatively, assembling asymmetric SCs using aqueous electrolytes is said to be an effective way to broaden the working potential of SCs. The capacity of a SC is depending on the intrinsic properties of electrode materials, which includes chemical activities, surface area, conductivity and configuration[16, 17].

Since the capacitive performance of carbon-based electrode materials is limited by the electrostatic charge accumulation, thus, the continuous exploration has been allocated in using faradaic materials to provide capacity surge from the faradic redox reactions[4]. Among the various faradaic materials that have been reported, vanadium disulphide (VS_2) has shown promising electrochemical properties for high-performance SCs. Different from other layered transition metal dichalcogenides (WS_2 , CoS_2 and MoS_2), 2D layered VS_2 exhibits excellent intrinsic metallic conductivity[18-21]. Consequently, 2D layered VS_2 has been employed as the electrode materials in SCs[22-24]. Unfortunately, the bare VS_2

based electrode material shows limited capacity due to the decreased ion-accessible surface area and reduced kinetics caused by the restacked thick and bulky VS₂ layers. Compared to bulk VS₂, VS₂ ultrananosheets have been proven to have unparalleled properties such as large accessible surface area, high conductivity and great mechanical characteristic[25]. However, the disadvantage of nanosheets is attributed to its readily stacked property caused by strong van der Waals force, consequently reduces its surface active sites for electrochemical reaction[23]. An effective way to alleviate this problem is directly to grow the VS₂ nanosheets on a highly conductive backbone, to guarantee the good kinetics without compromising the accessible active sites. According to previous research, NiCo₂S₄ is a potential backbone to in situ grow VS₂ nanosheets due to the controllable morphology, high specific capacity and metal-like conductivity[26]. Aforementioned, the capacity is related to the morphology and configuration of the composite apart from the inherent quality of electrode materials[15, 16].

Herein, we demonstrated a new approach in synthesizing a free-standing electrode composed of NiCo₂S₄@VS₂ on Ni foam by facile hydrothermal method. The highly conductive NiCo₂S₄ nanoneedle arrays grown on the Ni foam was then used as the scaffold to in situ grow ultrathin VS₂ nanosheets. In this free-standing nanostructured composites, faradaic NiCo₂S₄ needles not only prevent the restacking of VS₂ nanosheets, but also act as super-high-way for charge transfer channels. Moreover, the highly conductive VS₂ nanosheets grafted on NiCo₂S₄ needles further provide enhanced electrochemical performance. Therefore, the prepared NiCo₂S₄@VS₂ nanostructured electrode material exhibited a specific capacity of 1023.4 mAh g⁻¹ in a three-electrode system. At a two-electrode system, the asymmetric supercapacitor possessed good stabilities under different current densities, coupled with a high energy of 31.2 Wh kg⁻¹ at the power densities of 775 W kg⁻¹ in a wide potential window of 1.55 V.

2. Experimental

2.1. Reagents and materials

Sodium orthovanadate (Na₃VO₄·12H₂O), nickel chloride (NiCl₂·6H₂O), cobalt chloride

($\text{CoCl}_2 \cdot 6\text{H}_2\text{O}$), thioacetamide (TAA), ammonium fluoride (NH_4F), potassium hydroxide (KOH), polytetrafluoroethylene (PTFE) and other organic solvents were obtained from Wako (Japan). Active carbon (AC) and carbon black (50% compressed, $75 \text{ m}^2/\text{g}$, 80-120 g/L) were purchased from Alfa Aesar, American. Nickel foam (thickness: 1 mm) was purchased from Suzhou zhongditai metal material Co. LTO, china. All the analytical grade reagents were used without further purification.

2.2. Synthesis of VS_2

Typically, 3 mmol $\text{Na}_3\text{VO}_4 \cdot 12\text{H}_2\text{O}$ and 15 mmol TAA were dissolved in 40 mL deionized water and magnetically stirred to form a dark green solution. Then, the homogeneous solution was transferred to a 50 mL Teflon-lined stainless steel autoclave (TLSSA). The TLSSA was then sealed and maintained at $160 \text{ }^\circ\text{C}$ for 24 h. After cooling to room temperature, the obtained black precipitate was filtered and washed several times. Subsequently, the black powder was dried in a vacuum oven at $60 \text{ }^\circ\text{C}$ for 24 h. Finally, the powder was annealed at $300 \text{ }^\circ\text{C}$ for 2 h.

2.3. Synthesis of NiCo_2S_4 and $\text{NiCo}_2\text{S}_4@/\text{VS}_2$ on Ni foam

Preparation of NiCo_2S_4 was referred to the previous report[26]. In a typical synthesis procedure, a transparent solution consists of 2 mmol $\text{NiCl}_2 \cdot \text{H}_2\text{O}$ and 4 mmol $\text{CoCl}_2 \cdot \text{H}_2\text{O}$ in 80 mL deionized water was first prepared. After this, 3 mmol NH_4F and 24 mmol urea were added into the solution. The solution and pretreated Ni foams were transferred into a 100 mL TLSSA for hydrothermal reaction at $100 \text{ }^\circ\text{C}$ for 5 h. After cooling to room temperature, the obtained Ni foam coated with pink color materials was washed by deionized water and ethanol under sonication. To prepare NiCo_2S_4 , Ni foam coated with NiCo carbonate hydroxide was put into a TLSSA containing TAA for sulfurization reaction. The final NiCo_2S_4 product was washed by ethanol and deionized water, subsequently was dried in a vacuum oven at $60 \text{ }^\circ\text{C}$ for 24 h. To make $\text{NiCo}_2\text{S}_4@/\text{VS}_2$, TAA and Na_3VO_4 were magnetically stirred and transferred into a TLSSA containing NiCo precursors under the same reaction conditions. The fabricated sample was subsequently washed and dried before electrochemical test was carried out. Prior to the beginning,

Ni foams (3 cm×3.5 cm) were cleaned with 3 M HCl to remove the surficial nickel oxides, and then washed with ethanol and water individually. The average weight of Ni foam is 35.3 mg and the mass of positive electrode materials is 2.5 mg cm⁻², respectively.

2.4. Asymmetric supercapacitors (ASC)

The positive and negative supercapacitor electrodes were assembled, forming a sandwich structure separated by the polypropylene as the separator. The electrochemical performances of the ASC were conducted via two-electrode system using 3 M KOH as the electrolyte. The preparation of negative electrode is provided in Supplementary Materials. To achieve high supercapacitor performance, the mass of positive and negative electrodes were determined based on the charge balance theory shown as followings[15]:

$$\frac{m_+}{m_-} = \frac{C_- \times \Delta V_-}{C_+ \times \Delta V_+}$$

Where m (g), C and ΔV (V) are the active materials excluding the current collectors, specific capacity and working potential in three-electrode system.

2.5. Characterization

The material phases and structure were recorded by X-ray diffractometer employing Cu Ka radiation (XRD; RIGAKU, model D/max-2500 system at 40 kV in the 2theta range of 10°- 80°. The morphologies of the prepared electrode materials were characterized by a field effect scanning electron microscope (HITACHI, S-5200, Japan). The high-resolution transmission electron microscopy (HRTEM) images of the materials were observed with a JEM-F200 (JEOL) at 200 kV.

2.6. Electrochemical measurements

The electrochemical properties of the materials were recorded by a Solartron 1287 Potentiostat Galvanostat and 1255B Frequency Response Analyzer in a 3-electrode and 2-electrode systems. For the

3-electrode configuration, the as-prepared materials were used as working electrodes after sonication. Pt plate (2 cm×2 cm) and Hg/HgO were employed as counter and reference electrodes, respectively.

The specific capacity was calculated from the discharge curves according to the equation[8, 12]:

$$C_s = i \times \Delta t$$

where C_s is capacity (mAh g⁻¹), i and Δt present current density (A g⁻¹) and discharge time (s), severally.

The energy density (E) and power density (P) of the asymmetric SCs were determined from the following equations[2, 7, 27, 28]:

$$E = \frac{1}{2} CV^2$$

$$P = \frac{E}{\Delta t}$$

It should be pointed out that only mass of active materials of both positive and negative electrodes was used in the calculation of E and P in this work.

3. Results and Discussion

3.1. Material synthesis and characterization

Fig. 1 the synthesis illustration of NiCo₂S₄@VS₂

Fig. 1 illustrates the synthesis route of free-standing NiCo₂S₄@VS₂ nanorod arrays on a 3D sponge-like structure nickel foam with high specific surface area and superior electrical conductivity (Fig. S1). The formation of NiCo₂S₄@VS₂ active materials in an enclosed system of hydrothermal process happened where firstly, Ni²⁺ and Co²⁺ are co-precipitated with CO₃²⁻ and OH⁻ (released from urea), thus form NiCo carbonate hydroxide needle arrays grown on Ni foam in the hydrothermal reaction[26, 28]. The needle arrays of NiCo possess high surface area, which enable the anchoring of ultrathin VS₂ sheets in the subsequent temperature-controlled hydrothermal process. While the TAA used to synthesize VS₂ converts NiCo carbonate hydroxide to NiCo₂S₄. Finally, a highly conductive and accessible faradaic's

active sites NiCo₂S₄@VS₂ composite was successfully synthesized and is highly desirable for high performance SCs applications. Consequently, the tedious process to synthesize multicomponent electrode materials can be avoided without compromising electrochemical properties in the strategy.

Fig. 2 XRD patterns of VS₂ (red line), NiCo₂S₄ (blue line) and NiCo₂S₄@VS₂ (black line)

XRD was performed to investigate the crystallinities and phase structures of the obtained VS₂, NiCo₂S₄ and NiCo₂S₄@VS₂. The strong diffraction peaks located at 15.3°, 35.7°, 45.2° and 57.2° (red line) are indexed to (001), (011), (012) and (110) planes, indicating the hexagonal 1T phase of VS₂ (JCPDS card No. 01-089-1640)[17, 18, 23]. In addition, the strong and sharp peak situated at 15.3° suggests the lamellar stacking feature of the as-prepared VS₂[24]. The strong peaks at 31.5°, 38.2°, 50.4° and 55.2° (blue line) are corresponded to (311), (400), (511) and (440) planes of cubic NiCo₂S₄, while the high intensity Ni foam peaks are located at peaks 44.5°, 52.0° and 76.6°[15, 26, 29]. Notably, all the remarkable peaks can be successfully indexed to either VS₂ or NiCo₂S₄, apart from the 3 strong peaks of nickel foams. Thereby, NiCo₂S₄@VS₂ was successfully synthesized, as proven through the XRD profile.

Fig. 3 FESEM and HRTEM of NiCo₂S₄ (a, b, c) and NiCo₂S₄@VS₂ (d, e, f)

The morphologies of NiCo₂S₄ and NiCo₂S₄@VS₂ (Fig. 3) were observed via FESEM. Apparently, the Ni foam has been fully covered by the needle arrays of NiCo₂S₄, as shown in Fig. 3a and b. The thin and long (about 100 nm in diameter and over 1 μm in length) NiCo₂S₄ (Fig. 3c) needles provide a favourable condition for in situ growing of VS₂ tiny sheets, as exhibited in Fig. 3c. Compared to NiCo₂S₄, the nanorod arrays of NiCo₂S₄@VS₂ nanostructured composite are still remained. The twining of VS₂ nanosheets along the NiCo₂S₄ needle arrays has subtly changed the morphology of NiCo₂S₄@VS₂ to furry-like structure, as manifested in Fig. 3d and e. Interestingly, the alteration of VS₂ bulk stacking

layers (Fig. S2) to nanosheets was due to NiCo₂S₄ needle arrays, which effectively alleviate the stacking of the VS₂ layers. The rough and compact fur-like NiCo₂S₄@VS₂ structure was also presented in Fig. 3f (TEM image), suggesting large amount of active sites and efficient charge transfer channels for redox reaction.

3.2. Electrochemical properties (three-electrode system)

Series and systematic studies on three-electrode configured electrochemical evaluations such as cyclic voltammetry (CV), galvanostatic charge/discharge (GCD), and cyclic stability measurements were firstly conducted for VS₂, NiCo₂S₄, and NiCo₂S₄@VS₂ supercapacitor electrodes, respectively.

Fig. 4 Electrochemical performance of VS₂: (a) CV curves at various scanning rates; (b) GCD curves under different current densities; (c) specific capacities at different current densities; (d) cycle performance at a current density of 0.45 A g⁻¹

Fig 4a shows the CV curves of VS₂ electrode at various scan rates. It shows that there are no obvious changes on the CV pattern as the scan rate increases. However, a pair of redox peaks observed in CVs (Fig. 4a), implies its faradaic behavior. Therefore, the oxidation peaks and reduction peaks due to the reversible transformation of V^{6+/5+}/V⁴⁺[30]. Due to internal resistance and polarization effect, the reduction and oxidation peaks, both are shifted to more negative and more positive regions, respectively, in conjunction with the increasing scan rates[3, 29, 31]. As depicted in Fig. 4b, all GCD curves present symmetry platforms, which is consistent with the CV patterns. The specific capacities of the VS₂ electrode under different current densities were calculated based on equation of $C = i \times \Delta t$ and the relations between current density (x-axis) and specific capacity (y-axis) were plotted, as shown in Fig. 4c. It shows that the maximum specific capacity is less than 110 mAh g⁻¹ at the smallest current density, which may be due to the stacking layers of bulky VS₂ (as observed in Fig. S2). In addition, it shows that the specific capacity decreases with increasing current density owing to insufficient time for the electrolyte ions to diffuse throughout the VS₂ electrode at high current densities. Fig. 4d manifests the

well-maintained cyclic retention of VS₂ electrode where 96% of its original capacity was retained after 1000 charge discharge cycles, thus demonstrates its potential to be applied for supercapacitor applications.

Fig. 5 Electrochemical performance of NiCo₂S₄: (a) CV curves at various scanning rates; (b) GCD curves under different current densities; (c) specific capacities at different current densities; (d) cycle performance at a current density of 1.125 A g⁻¹

The electrochemical performances of NiCo₂S₄ electrode were evaluated. The representative CV (Fig. 5a) and GCD (Fig. 5b) profiles show no different against the VS₂ electrode. The apparent peaks and well-defined plateaus in CV (Fig. 5a) and GCD (Fig. 5b) suggest its capacity is mainly from redox reaction[31].

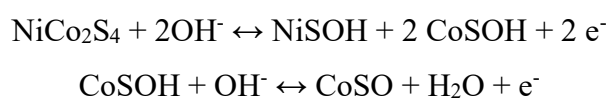


Fig. 5c shows the plot of calculated specific capacities at various current densities. At a current density of 0.45 A g⁻¹, the NiCo₂S₄ electrode achieved high specific capacity of 588.1 mAh g⁻¹, whereas the specific capacity dropped to 468 mAh g⁻¹ at a high current density of 4.5 A g⁻¹ due to inadequate response time for the electrolyte ions to reach the active surface of the materials at high current density. Interestingly, NiCo₂S₄ supercapacitor electrode exhibited remarkable stability (110% capacity retained) after 2000 cycle. A slight decrease in specific capacity for the first 500 cycles could be attributed to the loosely bonded active materials on the Ni foam upon sonication process before electrochemical performances were conducted. Subsequently, the increase in specific capacity might be contributed to activation process and complete wetting of the electrode[3]. The high capacity and good stability of NiCo₂S₄ as well as the conductive needle arrays verify its feasibility as an ideal scaffold for in situ growing VS₂ nanosheets.

Fig. 6 Electrochemical performance of NiCo₂S₄@VS₂: (a) CV curves at various scanning rates; (b) GCD curves at different current densities; (c) specific capacities at different current densities; (d) cycle performance at a current density of 0.675 A g⁻¹

Fig. 6 depicts the electrochemical properties of NiCo₂S₄@VS₂ composite electrode measured through CV (Fig. 6a), GCD (Fig. 6b), and cyclic retention (Fig. 6d) in a three-electrode system. The redox peaks and platforms of NiCo₂S₄@VS₂ are from the reversible processes of V⁶⁺/V⁵⁺/V⁴⁺, Ni²⁺/Ni³⁺, Co²⁺/Co³⁺ and Co³⁺/Co⁴⁺ transitions. Fig. S4a presents the CV curves of VS₂, NiCo₂S₄, and NiCo₂S₄@VS₂ at the same scanning rate in the potential range of 0-0.65 V. It shows that NiCo₂S₄@VS₂ electrode material exhibited larger voltammogram area than VS₂ and NiCo₂S₄ active materials, suggesting the best charge storage performance. As given in Fig. S4b, the nanostructured composite has achieved a high specific capacity of 1023.4 mAh g⁻¹ at current density of 0.45 A g⁻¹, which is about 1.7-fold and 9.8-fold higher than separate NiCo₂S₄ and VS₂ electrodes, respectively owing to longer discharging time of 2275 s, as illustrated in Fig. S4b. At higher current density of 4.5 A g⁻¹, the specific capacity of composite NiCo₂S₄@VS₂ could still retained at 715 mAh g⁻¹, implies good rate capability (Fig. 6c). Fig. 6d shows the cyclic performance of NiCo₂S₄@VS₂ electrode material at current density of 0.675 A g⁻¹. The gradual increasing in specific capacity for the first 1000 cycles is due to the activation process in the electrode. As the charge discharge cycles increases, the gradual decrement in specific capacity could be resulted from electrode deterioration, which attributed to extensive expansion and contraction of the electrodes during the charge discharge process. Overall, the NiCo₂S₄@VS₂ electrode possesses excellent stability up to 96% capacity retained upon 2000 cycles, indicative of its high recyclability and reversibility of the electrode materials.

Fig. 7 Schematic illustration of charge storage and transfer merits of NiCo₂S₄@VS₂

The schematic illustration of NiCo₂S₄@VS₂ is exhibited in Fig. 7 and the advantages of depositing NiCo₂S₄@VS₂ on nickel foam: **(1) large accessible surface area for redox reaction** where in situ

growing of NiCo₂S₄ needle arrays on conductive 3D sponge-like Ni foams provide ample active sites for grafting of VS₂ nanosheets; compared to stacked and bulky bare VS₂, the ultrathin VS₂ nanosheets supported on NiCo₂S₄ resulted in larger surface area[32-34]. **(2) Excellent charge transfer and shorter diffusion path.** It is known that NiCo₂S₄ has metal-like conductive property, which is ideal for charge transfer. Additionally, synthesis of binder-free active materials directly grown on the Ni foam current collector further enhances its conductivity. Furthermore, nanostructure and abundant pores among intercrossed VS₂ nanosheets shorten the diffusion length and facilitates the penetration of electrolytes, resulted in an increased active site for redox reaction and greatly enhanced diffusion kinetics. **(3) Both of the NiCo₂S₄ and VS₂ possess faradaic features**, both of which contribute to the increased capacity. Additionally, the good mechanical adhesion among aforementioned materials further improves the stability. Therefore, the advantages of corresponding single components are maximally optimized, leading to the high capacity and good long-term stability.

3.3. Electrochemical performance of NiCo₂S₄@VS₂/AC asymmetric supercapacitors

Fig. 8 The assembled ASC: (a) schematic illustration of the device; (b) CV curves at different scanning rates; (c) GCD plots under various current densities; (d) Ragone plot and (d) cycle performance under different current densities

An ASC composed of NiCo₂S₄@VS₂ as the positive electrode and AC as the negative electrode separated by polypropylene membrane separator was fabricated to gauge the potential of the synthesized NiCo₂S₄@VS₂ material for practical application. The material loading for the ASC was determined based on the charge balance theory where the calculated mass ratio of NiCo₂S₄@VS₂ and AC is 2.5:4.2. Fig. 8a presents the schematic illustration of the as-assembled ASC. The positive electrode of ASC recorded a working potential from 0-0.55 V, while the negative electrode recorded a working potential from -1-0 V (Fig. S7), hence give rise to an operating potential window of 0-1.55 V. The CV curves (Fig. 8b) show a mixed feature of electric double layer and faradaic reaction without any observable distortion,

implying its excellent charge transport ability and rate capability. The triangular GCD profiles with plateaus obtained at various current densities further confirm its combined properties of double layer capacity and faradaic reaction. Fig. 8d illustrates the Ragone plot of ASC where the maximum energy density decrease from 31.2 Wh kg⁻¹ to 11.7 Wh kg⁻¹ when the power densities are increased from 775 W kg⁻¹ to 7750 W kg⁻¹, which are higher than other reported works[13, 15, 34-41]. Fig. 8e shows the cycle performance of device at various current densities. At the current density of 1.5 A g⁻¹, the capacity first maintained at 114.1 mAh g⁻¹ and slightly increased due to the activation process. Nevertheless, the capacity dropped at high current density of 5 Ag⁻¹, which may be resulted from the insufficient response time for the electrolyte ions to intercalate and de-intercalate from the surface of supercapacitor electrode at a high current density. Interestingly, the capacity simultaneously reverts to about 80.4 mAh g⁻¹ when the current density returns to 3 A g⁻¹. All in all, the impressive electrochemical performances of NiCo₂S₄@VS₂ based asymmetric supercapacitors show its great potential for practical energy storage system and future commercialization.

4. Conclusions

We have successfully prepared NiCo₂S₄@VS₂ nanorod arrays on Ni foam by facile in situ sulfurization-assisted hydrothermal process and its electrochemical performances either in three-electrode or two-electrode system were investigated. The NiCo₂S₄@VS₂ electrode materials exhibited a high specific capacity of 1023.4 mAh g⁻¹ at a current density of 0.45 Ag⁻¹ and excellent stability performance upon 2000 charge discharge cycles. When the NiCo₂S₄@VS₂ positive electrode was coupled to an activated carbon negative electrode, the ASC presented a high energy density of 31.2 Wh kg⁻¹ at power densities of 775 W kg⁻¹, respectively, without compromising its cyclic stability performance. In conclusion, the as-synthesized NiCo₂S₄@VS₂ active materials have the potential to be used as electrode materials for real supercapacitor application owing to its excellent cyclic stability and charge storage ability.

Acknowledgments

This work was supported by the Grant-in-Aid for Scientific Research (KAKENHI) program, Japan (C, Grant Number 15K05597), Takahashi Industrial and Research Center for Solar Light Energy Conversion, Kyushu Institute of Technology.

References

- [1] A. González, E. Goikolea, J.A. Barrena, R. Mysyk, Review on supercapacitors: technologies and materials, *Renewable and Sustainable Energy Reviews*, 58 (2016) 1189-1206.
- [2] X.-P. Gao, H.-X. Yang, Multi-electron reaction materials for high energy density batteries, *Energy & Environmental Science*, 3 (2010) 174-189.
- [3] X. Huang, Z. Zhang, H. Li, Y. Zhao, H. Wang, T. Ma, Novel fabrication of Ni₃S₂/MnS composite as high performance supercapacitor electrode, *Journal of Alloys and Compounds*, 722 (2017) 662-668.
- [4] L. Wang, H. Yang, T. Shu, X. Chen, Y. Huang, X. Hu, Rational Design of Three-Dimensional Hierarchical Nanomaterials for Asymmetric Supercapacitors, *ChemElectroChem*, 4 (2017) 2428-2441.
- [5] B.E. Conway, Transition from “supercapacitor” to “battery” behavior in electrochemical energy storage, *Journal of the Electrochemical Society*, 138 (1991) 1539-1548.
- [6] H. Zhou, L. Zhang, D. Zhang, S. Chen, P.R. Coxon, X. He, M. Coto, H.-K. Kim, K. Xi, S. Ding, A universal synthetic route to carbon nanotube/transition metal oxide nano-composites for lithium ion batteries and electrochemical capacitors, *Scientific reports*, 6 (2016) 1-11.
- [7] J. Zhu, S. Tang, J. Wu, X. Shi, B. Zhu, X. Meng, Wearable High-Performance Supercapacitors Based on Silver-Sputtered Textiles with FeCo₂S₄-NiCo₂S₄ Composite Nanotube-Built Multitripod Architectures as Advanced Flexible Electrodes, *Advanced Energy Materials*, 7 (2017) 1-11.
- [8] J.R. Miller, P. Simon, Electrochemical capacitors for energy management, *Science Magazine*, 321 (2008) 651-652.
- [9] L. Lin, S. Tang, S. Zhao, X. Peng, N. Hu, Hierarchical three-dimensional FeCo₂O₄@ MnO₂ core-shell nanosheet arrays on nickel foam for high-performance supercapacitor, *Electrochimica Acta*, 228 (2017) 175-182.
- [10] M.R. Lukatskaya, B. Dunn, Y. Gogotsi, Multidimensional materials and device architectures for future hybrid energy storage, *Nature communications*, 7 (2016) 1-13.
- [11] Y. Yang, D. Cheng, S. Chen, Y. Guan, J. Xiong, Construction of hierarchical NiCo₂S₄@ Ni(OH)₂ core-shell hybrid nanosheet arrays on Ni Foam for high-performance aqueous hybrid supercapacitors, *Electrochimica Acta*, 193 (2016) 116-127.
- [12] H. Gao, S. Cao, Y. Cao, Hierarchical Core-Shell Nanosheet Arrays with MnO₂ Grown on Mesoporous CoFe₂O₄ Support for High-Performance Asymmetric Supercapacitors, *Electrochimica Acta*, 240 (2017) 31-42.
- [13] S. Wen, Y. Liu, F. Zhu, R. Shao, W. Xu, Hierarchical MoS₂ nanowires/NiCo₂O₄ nanosheets supported on Ni foam for high-performance asymmetric supercapacitors, *Applied Surface Science*, 428 (2018) 616-622.
- [14] Z. Zhang, Y. He, Q. Zhou, C. Huang, X. Zhang, Z. Guo, Y. Gao, J. Liu, Z. Cao, Unique Ni@ NiO core-shell/AC composite for supercapacitor electrodes, *Electrochimica Acta*, 144 (2014) 300-306.
- [15] Z. Zhang, X. Huang, H. Li, H. Wang, Y. Zhao, T. Ma, All-solid-state flexible asymmetric supercapacitors with high energy and power densities based on NiCo₂S₄@ MnS and active carbon, *Journal of Energy Chemistry*, 26 (2017) 1260-1266.
- [16] A.S. Aricò, P. Bruce, B. Scrosati, J.-M. Tarascon, W. Van Schalkwijk, Nanostructured materials for advanced energy conversion and storage devices, *Nature materials*, 4 (2005) 366-377.
- [17] A. Maitra, A.K. Das, R. Bera, S.K. Karan, S. Paria, S.K. Si, B.B. Khatua, An Approach To Fabricate PDMS Encapsulated All-Solid-State Advanced Asymmetric Supercapacitor Device with Vertically Aligned Hierarchical Zn-Fe-Co Ternary Oxide Nanowire and Nitrogen Doped Graphene Nanosheet for High Power Device Applications, *ACS applied materials & interfaces*, 9 (2017) 5947-5958.
- [18] H. Liang, H. Shi, D. Zhang, F. Ming, R. Wang, J. Zhuo, Z. Wang, Solution Growth of Vertical VS₂ Nanoplate Arrays for Electrocatalytic Hydrogen Evolution, *Chemistry of Materials*, 28 (2016) 5587-5591.
- [19] Y. Qu, M. Shao, Y. Shao, M. Yang, J. Xu, C.T. Kwok, X. Shi, Z. Lu, H. Pan, Ultra-high electrocatalytic activity of VS₂ nanoflowers for efficient hydrogen evolution reaction, *Journal of Materials Chemistry A*, 5 (2017) 15080-15086.
- [20] C. Song, K. Yu, H. Yin, H. Fu, Z. Zhang, N. Zhang, Z. Zhu, Highly efficient field emission properties of a novel layered VS₂/ZnO nanocomposite and flexible VS₂ nanosheet, *Journal of Materials Chemistry C*, 2 (2014) 4196-4202.
- [21] N. Li, T. Lv, Y. Yao, H. Li, K. Liu, T. Chen, Compact graphene/MoS₂ composite films for highly flexible and stretchable all-solid-state supercapacitors, *Journal of Materials Chemistry A*, 5 (2017) 3267-3273.
- [22] J. Feng, X. Sun, C. Wu, L. Peng, C. Lin, S. Hu, J. Yang, Y. Xie, Metallic few-layered VS₂ ultrathin nanosheets: high two-dimensional conductivity for in-plane supercapacitors, *Journal of the American Chemical Society*, 133 (2011) 17832-17838.
- [23] R. Sun, Q. Wei, J. Sheng, C. Shi, Q. An, S. Liu, L. Mai, Novel layer-by-layer stacked VS₂ nanosheets with intercalation pseudocapacitance for high-rate sodium ion charge storage, *Nano Energy*, 35 (2017) 396-404.
- [24] M. van den Hoop, J. Benegas, Colloids and surfaces a: physicochemical and engineering aspects, *Colloids and Surfaces A: Physicochemical and Engineering Aspects*, 170 (2000) 151-160.
- [25] L. Zhou, H. Cao, S. Zhu, L. Hou, C. Yuan, Hierarchical micro-/mesoporous N- and O-enriched carbon derived from disposable cashmere: a competitive cost-effective material for high-performance electrochemical capacitors, *Green Chemistry*, 17 (2015) 2373-2382.
- [26] Z. Zhang, X. Huang, H. Li, Y. Zhao, T. Ma, 3-D honeycomb NiCo₂S₄ with high electrochemical performance used for supercapacitor electrodes, *Applied Surface Science*, 400 (2017) 238-244.
- [27] P. Asen, S. Shahrokhian, A High Performance Supercapacitor Based on Graphene/Polypyrrole/Cu₂O-Cu (OH)₂ Ternary Nanocomposite Coated on Nickel Foam, *The Journal of Physical Chemistry C*, 121 (2017) 6508-6519.
- [28] J.-G. Wang, D. Jin, R. Zhou, C. Shen, K. Xie, B. Wei, One-step synthesis of NiCo₂S₄ ultrathin nanosheets on conductive substrates as advanced electrodes for high-efficient energy storage, *Journal of Power Sources*, 306 (2016) 100-106.
- [29] L. Niu, Y. Wang, F. Ruan, C. Shen, S. Shan, M. Xu, Z. Sun, C. Li, X. Liu, Y. Gong, In situ growth of NiCo₂S₄@ Ni₃V₂O₈ on Ni foam as a binder-free electrode for asymmetric supercapacitors, *Journal of Materials Chemistry A*, 4 (2016) 5669-5677.
- [30] Y. Zhang, W. Sun, X. Rui, B. Li, H.T. Tan, G. Guo, S. Madhavi, Y. Zong, Q. Yan, One-Pot Synthesis of Tunable Crystalline Ni₃S₄@ Amorphous MoS₂ Core/Shell Nanospheres for High-Performance Supercapacitors, *Small*, 11 (2015) 3694-3702.
- [31] J. Wang, J. Polleux, J. Lim, B. Dunn, Pseudocapacitive contributions to electrochemical energy storage in TiO₂ (anatase) nanoparticles, *The Journal of Physical Chemistry C*, 111 (2007) 14925-14931.
- [32] J. Liang, K. Xi, G. Tan, S. Chen, T. Zhao, P.R. Coxon, H.-K. Kim, S. Ding, Y. Yang, R.V. Kumar, Sea urchin-like NiCoO₂@ C nanocomposites for Li-ion batteries and supercapacitors, *Nano Energy*, 27 (2016) 457-465.
- [33] M. Wang, X. Zhang, Three - Dimensional Co₃O₄@ NiCo₂S₄ Core/Shell Nanoflower Array with Enhanced Electrochemical Performance, *ChemistrySelect*, 2 (2017) 9537-9545.
- [34] Y. Yuan, W. Wang, J. Yang, H. Tang, Z. Ye, Y. Zeng, J. Lu, Three-Dimensional NiCo₂O₄@ MnMoO₄ Core-Shell Nanoarrays for High-Performance Asymmetric Supercapacitors, *Langmuir*, 33 (2017) 10446-10454.
- [35] X. Xiong, G. Waller, D. Ding, D. Chen, B. Rainwater, B. Zhao, Z. Wang, M. Liu, Controlled synthesis of NiCo₂S₄ nanostructured arrays on carbon fiber paper for high-performance pseudocapacitors, *Nano Energy*, 16 (2015) 71-80.

- [36] Y. Liu, G. Jiang, S. Sun, B. Xu, J. Zhou, Y. Zhang, J. Yao, Decoration of carbon nanofibers with NiCo₂S₄ nanoparticles for flexible asymmetric supercapacitors, *Journal of Alloys and Compounds*, 731 (2018) 560-568.
- [37] Y. Liu, G. Jiang, S. Sun, B. Xu, J. Zhou, Y. Zhang, J. Yao, Growth of NiCo₂S₄ nanotubes on carbon nanofibers for high performance flexible supercapacitors, *Journal of Electroanalytical Chemistry*, 804 (2017) 212-219.
- [38] Z. Wu, X. Pu, X. Ji, Y. Zhu, M. Jing, Q. Chen, F. Jiao, High Energy Density Asymmetric Supercapacitors From Mesoporous NiCo₂S₄ Nanosheets, *Electrochimica Acta*, 174 (2015) 238-245.
- [39] W. Kong, C. Lu, W. Zhang, J. Pu, Z. Wang, Homogeneous core-shell NiCo₂S₄ nanostructures supported on nickel foam for supercapacitors, *Journal of Materials Chemistry A*, 3 (2015) 12452-12460.
- [40] Y. Zhu, Z. Wu, M. Jing, X. Yang, W. Song, X. Ji, Mesoporous NiCo₂S₄ nanoparticles as high-performance electrode materials for supercapacitors, *Journal of Power Sources*, 273 (2015) 584-590.
- [41] Y. Zhu, X. Ji, Z. Wu, Y. Liu, NiCo₂S₄ hollow microsphere decorated by acetylene black for high-performance asymmetric supercapacitor, *Electrochimica Acta*, 186 (2015) 562-571.